

Reprinted from

JAPANESE JOURNAL OF
**APPLIED
PHYSICS**

REGULAR PAPER

**Improvement in Accuracy of Ultrasonic Measurement of Transient Change
in Viscoelasticity of Radial Arterial Wall Due to Flow-Mediated Dilation
by Adaptive Low-Pass Filtering**

Kazuki Ikeshita, Hideyuki Hasegawa, and Hiroshi Kanai

Jpn. J. Appl. Phys. **51** (2012) 07GF14

Improvement in Accuracy of Ultrasonic Measurement of Transient Change in Viscoelasticity of Radial Arterial Wall Due to Flow-Mediated Dilation by Adaptive Low-Pass Filtering

Kazuki Ikeshita¹, Hideyuki Hasegawa^{1,2}, and Hiroshi Kanai^{1,2*}

¹Graduate School of Biomedical Engineering, Tohoku University, Sendai 980-8579, Japan

²Graduate School of Engineering, Tohoku University, Sendai 980-8579, Japan

Received November 18, 2011; accepted February 27, 2012; published online July 20, 2012

In our previous study, the stress–strain relationship of the radial arterial wall was measured and the viscoelasticity of the intima–media region was estimated from the stress–strain relationship. Furthermore, the transient change in viscoelasticity due to flow-mediated dilation (FMD) was estimated by the automated detection of wall boundaries. In the present study, the strain rate was adaptively filtered to improve the accuracy of viscoelasticity estimation by decreasing the high-frequency noise. Additionally, in a basic experiment, this method was validated using a silicone tube (simulating artery). In the basic experiment, the elasticity was estimated with a mean error of 1.2%. The elasticity measured at each beam position was highly reproducible among measurements, whereas there was a slight variation in measured elasticity among beams. Consequently, in *in vivo* measurements, the normalized mean square error (MSE) was clearly decreased. Additionally, the stress–strain relationship of the radial arterial wall was obtained and the viscoelasticity was estimated accurately. The inner small loop, which corresponds to the negative pressure wave caused by the closure of the aortic valve, can be observed using the adaptive low-pass filtering (LPF). Moreover, the transient changes in these parameters were similar to those in the previous study. These results show the potential of the proposed method for the thorough analysis of the transient change in viscoelasticity due to FMD. © 2012 The Japan Society of Applied Physics

1. Introduction

Medical ultrasound is clinically used to make a diagnosis for various organs, and it can be repeatedly employed to confirm time-dependent changes of the targeted organs, because it is noninvasive and relatively stress-free for patients. Ultrasound B-mode imaging is widely used for the morphological diagnosis of the arterial wall. Additionally, as well as the morphology of the arterial wall, the viscoelasticity of the arterial wall and the condition of blood are also useful markers for the diagnosis of atherosclerosis.^{1–6)}

The quantitative assessment of atherosclerosis, which is the main cause of circulatory diseases, is essential for making an early diagnosis of such diseases. The endothelial dysfunction is considered to be an initial step of atherosclerosis.^{7,8)} Additionally, it has been reported that the smooth muscle, which constructs the media of the artery, changes its characteristics owing to atherosclerosis.⁹⁾ Consequently, it is important for an early preventive treatment to noninvasively assess the arterial wall properties, which are the endothelial function and the mechanical property of the media.

The arterial wall is composed of three layers, namely, intima, media and adventitia, as shown in Fig. 1.¹⁰⁾ The intima, the innermost layer, is composed of endothelial cells and an internal elastic layer. Endothelial cells react to the shear stress caused by blood flow and produce nitric oxide (NO), which is known as a vasodepressor material. The smooth muscle, which constructs the media, is the main source of the viscoelasticity of the vessel wall. Therefore, the dilation and contraction of the artery depend on the characteristics of the media. The smooth muscle is relaxed as a result of the response to the produced NO. This function is important for maintaining the homeostasis of the vascular system.¹¹⁾

For the evaluation of the endothelial function, there is a conventional technique for measuring the transient change in the inner diameter of the brachial artery caused by flow-

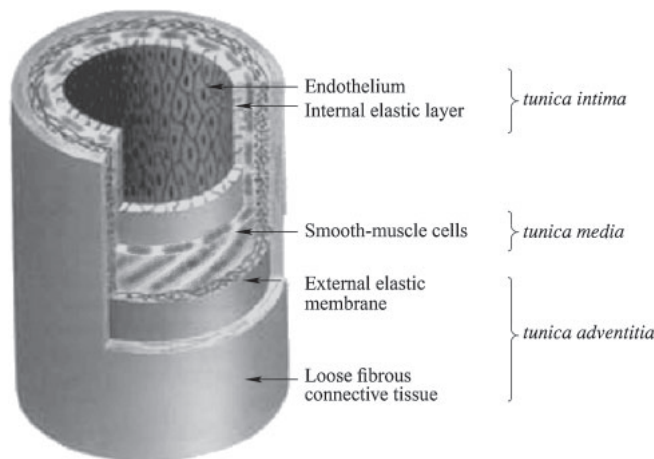


Fig. 1. Scheme of the arterial wall structure.⁴⁾

mediated dilation (FMD) after the release of avascularization.^{12–16)} FMD, which is the ratio of the change in diameter due to FMD to the original diameter, is related to the cardiovascular risk factor, such as the cerebral infarction and diabetes, and, thus, it is considered to be a reference index of circulatory diseases.^{17–19)} However, this method cannot directly evaluate the mechanical properties of the arterial wall.

For a more sensitive and detailed evaluation of the endothelial function and mechanical property of the media, we have proposed a new noninvasive method for the measurement of the elasticity of the brachial artery^{20,21)} and the stress–strain relationship of the radial arterial wall.²²⁾ Additionally, the viscoelasticity of the intima–media region was estimated from the stress–strain relationship.²³⁾ In our previous study, the transient change in viscoelasticity due to FMD was estimated by the automated detection of wall boundaries²⁴⁾ to reduce the operator dependence.

In the proposed method, it is necessary to measure viscoelasticity accurately and reproducibly to evaluate the rate of change in viscoelasticity after avascularization.

*E-mail address: hasegawa@ecei.tohoku.ac.jp

Therefore, in the present study, the strain rate was adaptively filtered to improve the accuracy of viscoelasticity estimation, by decreasing the high-frequency noise amplified by the differentiation of the strain. Additionally, the proposed method was validated using a silicone tube (simulating artery) by evaluating the accuracy of the estimation of viscoelasticity. Consequently, the proposed method was applied to the human radial artery and the transient change in viscoelasticity due to FMD was measured.

2. Principles and Experimental Methods

2.1 Principles of estimating artery wall viscoelasticity from measured stress–strain relationship and decreasing high-frequency noise by filtering

The detailed analysis of the change in the viscoelasticity of the arterial wall due to FMD requires the *in vivo* measurement of the stress–strain relationship, which has not been measured noninvasively thus far.

For the radial artery, the inner pressure can be non-invasively and continuously measured with a special sphygmometer (Colin JENTOW-7700). Thus, the waveform of blood pressure $p(t)$ can be obtained, and the viscoelasticity can be estimated from the stress–strain relationship.^{22–24)}

To determine the stress–strain relationship, the minute change in the thickness (radial strain) $\Delta h(t)$ of the right radial arterial wall during a cardiac cycle was also measured using the phased tracking method.²⁵⁾ Together with the measurement of ultrasonic RF signals for the estimation of $\Delta h(t)$, the waveform of blood pressure (stress) $p(t)$ in the left radial artery was continuously measured with the sphygmometer.

For the measurement of the change in thickness, the velocities of artery wall boundaries [namely, the lumen-intima boundary (LIB) and media-adventitia boundary (MAB)] were estimated. These boundaries were detected by adaptive template matching¹⁵⁾ and these velocities $v(t)$ were estimated from the phase shift $\Delta\theta(t)$ of RF echoes in two consecutive frames. The phase shift $\Delta\theta(t)$ was obtained using the complex cross-correlation applied to the quadrature demodulated signals of the measured RF echoes. The change in thickness, $\Delta h(t)$, between two different depths, A and B (corresponding to the LIB and MAB, respectively), in the arterial wall along an ultrasonic beam was obtained from the difference between the displacements $x_{LIB}(t)$ and $x_{MAB}(t)$ at these two positions as

$$\begin{aligned} \hat{h}(t) &= \hat{x}_{LIB}(t) - \hat{x}_{MAB}(t) \\ &= \int_0^t \int [\hat{v}_{LIB}(t) - \hat{v}_{MAB}(t)] dt. \end{aligned} \quad (1)$$

The strain $\gamma(t)$ was obtained from the change in thickness, $\Delta h(t)$, which is divided by the intima–media thickness at the time of the R-wave of the electrocardiogram. By assuming the Voigt model as a viscoelastic model of the intima–media region, the stress–strain relationship is given by

$$\hat{\tau}(t) = E_s \cdot \gamma(t) + \eta \cdot \dot{\gamma}(t) + \tau_0, \quad (2)$$

where $\hat{\tau}(t)$ is the stress modeled by the Voigt model, and $\gamma(t)$, $\dot{\gamma}(t)$, E_s , and η are the strain, strain rate, static elasticity, and viscosity coefficient, respectively. In the *in vivo* measurement, the measured stress $\tau(t)$ is the incremental strain due to the pulse pressure, whereas the measured stress

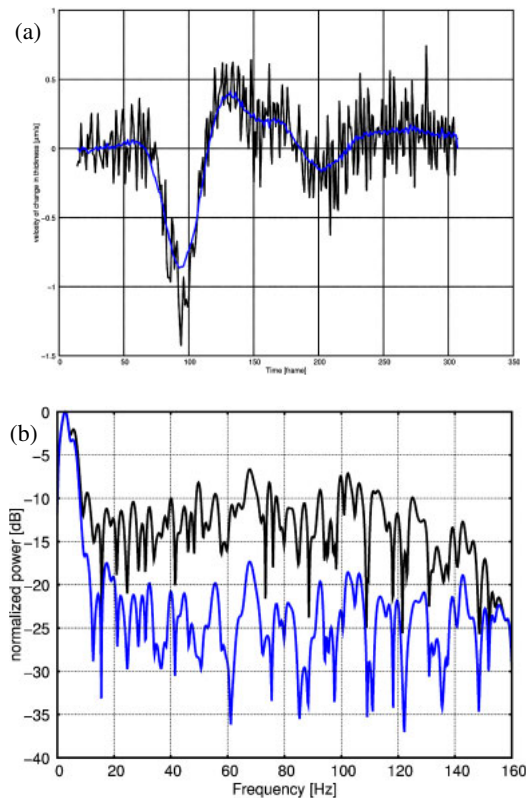


Fig. 2. (Color online) (a) Waveforms and (b) power spectra of strain rates of the arterial walls obtained with (blue) and without (black) filtering.

includes the bias stress (diastolic blood pressure). Therefore, τ_0 is added to the right-hand side of eq. (2) as the bias stress corresponding to the diastolic pressure.

In this study, the strain rate was filtered to decrease the high-frequency noise amplified by the differentiation of the strain. Figures 2(a) and 2(b) show the waveforms and spectra of the strain rates of the arterial walls obtained with and without filtering. By a low-pass filtering (LPF), the eq. (2) was rewritten by

$$\hat{\tau}_{LPF}(t) = E_s \cdot \gamma(t) + \eta \cdot LPF[\dot{\gamma}(t)] + \tau_0. \quad (3)$$

The mean square error (MSE) α between the measured $\tau(t)$ and model $\hat{\tau}_{LPF}(t)$ stresses is defined by

$$\alpha = E_t[\{\tau(t) - \hat{\tau}_{LPF}(t)\}^2], \quad (4)$$

where $E_t[\cdot]$ indicates the averaging operation during a cardiac cycle. The parameters in eq. (3), E_s , η , and τ_0 , were estimated by the least-squares method by minimizing the normalized MSE α between the measured and model stresses $\tau(t)$ and $\hat{\tau}_{LPF}(t)$. Additionally, the minimized MSE α_{min} was calculated at each cutoff frequency f_c of LPF in the range from 5 to 160 Hz, and the cutoff frequency, which gave minimum α_{min} , was determined adaptively.

2.2 Procedure for basic experiment

In this study, we evaluated the accuracy of the estimation of viscoelasticity by a basic experiment using a silicone tube (simulating artery). The silicone tube (wall thickness: 1 mm; inner diameter: 8 mm) includes graphite powder as scatterers, and we applied pulsatile flow (simulating blood flow) for the induction of pulsatile change in wall thickness.

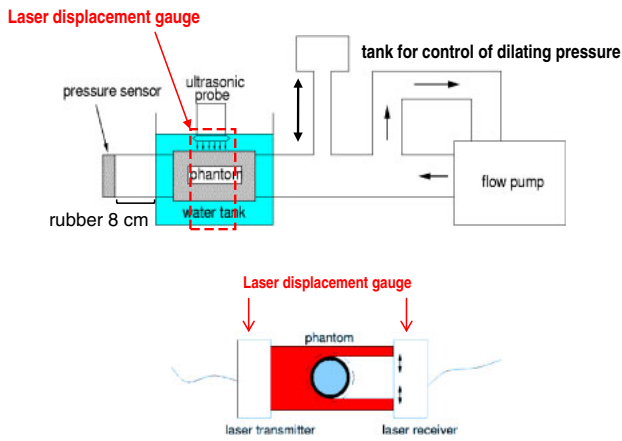


Fig. 3. (Color online) Basic experimental system.

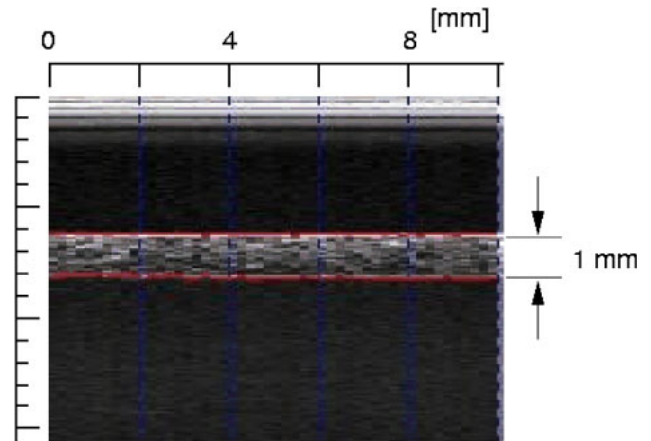


Fig. 4. (Color online) B-mode image of silicone tube.

In this experiment, we measured the changes in thickness and inner pressure caused by the pulsatile flow to obtain the stress–strain relationship, and the viscoelasticity was estimated using the principles described in §2.1. Additionally, for the evaluation of the accuracy of the proposed method, we estimated the elasticity of the silicone tube from the change in outer diameter, which was measured using a laser displacement gauge. Figure 3 shows the experimental system, and the elasticity, which was estimated using a laser, is defined by

$$E_{\text{inc}} = \frac{3}{2} \frac{d_0^2}{d_c^2 - d_0^2} \frac{\Delta p}{\Delta d_c(t)/d_c}, \quad (5)$$

where $\Delta d_c(t)$ and Δp indicate the changes in outer diameter and inner pressure, respectively. In the measurement using the laser displacement gauge, the apparatus employed in this study may have an undesirable time delay that would largely affect the estimation of the viscosity of the material. Therefore, we evaluated only the elasticity measured by ultrasound (E_s) by referring to the elasticity measured using a laser (E_{inc}).

2.3 Procedure for *in vivo* experiment

In this study, the right radial arteries of healthy subjects were measured. In this measurement, ultrasonic RF echoes (transmit center frequency: 22 MHz) were acquired at a sampling frequency of 66.5 MHz for 2 s at a frame rate of about 320 Hz. At the same time, the waveform of blood pressure on the left radial artery was continuously measured with a sphygmometer.

We applied this method to a healthy subject and evaluate the effect of filtering. Consequently, we measured the transient change in viscoelasticity due to FMD. This acquisition was repeated at every 20 s for 2 min at rest before avascularization and every 12 s for 3 min after recirculation.

3. Results

3.1 Results of basic experiment

For the validation of the method, we applied the proposed method to a silicone tube (simulating artery), and Fig. 4 shows the B-mode image of the anterior wall of the tube. We measured the change in the thickness of the anterior wall

caused by internal pulsatile flow (simulating blood flow). Figure 5 shows the results of the measurement of the change in the thickness of the silicone tube. In the basic experiment, the boundaries of the wall, which were tracked by the phase tracking method, were determined automatically by thresholding to the echo amplitude.

Additionally, in this measurement, the strain rate was filtered to decrease the high-frequency noise amplified by the differentiation of the strain. Figure 6 shows the effects of LPF. Figure 6(a) shows the α_{min} at each cutoff frequency f_c , and the adaptive cutoff frequency \hat{f}_c , which gives minimum α_{min} , is adaptively determined ($f_c = 20$ Hz in Fig. 6). Figure 6(b) shows the strain rates obtained with and without filtering using the adaptive cutoff frequency. Figures 6(c) and 6(d) show the estimated pressure and stress–strain relationship, respectively. As shown in Fig. 6(b), the high-frequency noise was clearly decreased, and α_{min} was decreased from 2.3 to 1.7%.

Moreover, for the evaluation of the accuracy of the proposed method, we estimated the elasticity of the silicone tube from the change in outer diameter, which was measured using the laser displacement gauge. Figure 7 shows the measured relationship between inner pressure and outer diameter (15 cycles of the pulsatile flow). The green line shows the mean measured elasticity (467 kPa), which was calculated using eq. (5).

Figure 8 shows the elasticity and viscosity of the silicone tube, which were estimated by the proposed method. In the ultrasound measurement, the mean elasticity was 472 kPa (mean viscosity was 8.67 kPa·s). The elasticity was estimated with a mean error of 1.2%.

3.2 Results of *in vivo* experiment

RF data for 2 s was obtained by each acquisition to include at least an entire cardiac cycle. Therefore, the changes in thickness and blood pressure were obtained for at least one cardiac cycle in each measurement for estimating the viscoelastic parameters of the radial arterial wall.

Figure 9 shows the effects of LPF in the *in vivo* measurement. As shown in Fig. 9(a), the normalized residual MSE α_{min} was decreased from 8.9 to 1.2% by adaptive LPF ($f_c = 12.3$ Hz). Figure 9(b) shows the measured and estimated pressures. Figure 9(c) shows the stress–

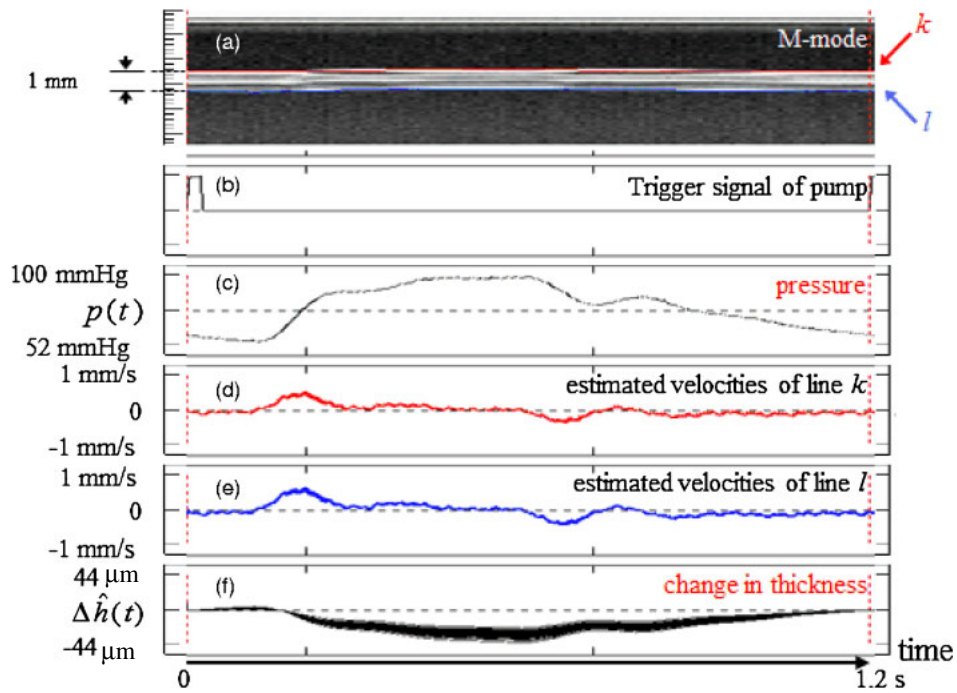


Fig. 5. (Color online) Results obtained for anterior wall of silicone tube (simulating artery). (a) M-mode image. (b) Trigger signal of pump. (c) Inner pressure. (d) Estimated velocities of line k . (e) Estimated velocities of line l . (f) Change in thickness.

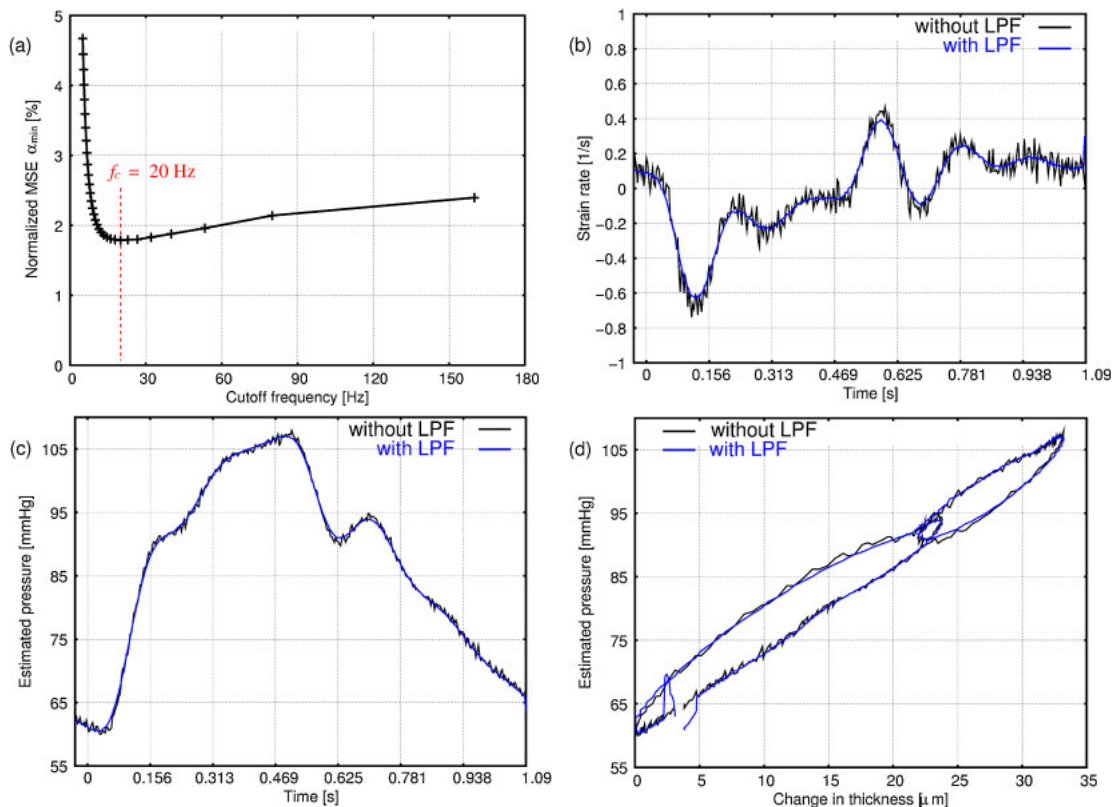


Fig. 6. (Color online) (a) Residual MSE α_{\min} at each cutoff frequency. (b) Strain rates obtained with and without filtering using adaptive cutoff frequency ($f_c = 20$ Hz). (c) Estimated pressure. (d) Stress–strain relationship.

strain relationship of the radial arterial wall during a heartbeat. The red line shows the hysteresis loop (reference) measured using a sphygmometer. The black and blue lines in Fig. 9(c) show the estimated loops obtained without and with filtering, respectively. Additionally, the inner small

loop, which corresponds to the negative pressure wave caused by the closure of the aortic valve, can be observed by adaptive LPF.

Figure 10 shows the transient change in α_{\min} between the measured and model stresses $\tau(t)$ and $\hat{\tau}_{LPF}(t)$. α_{\min} was

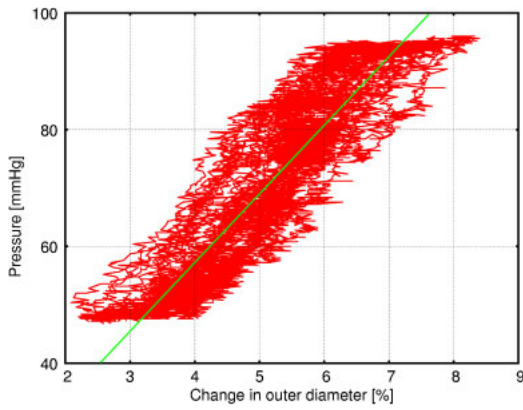


Fig. 7. (Color online) Relationship between inner pressure and outer diameter. A mean elasticity of 467 kPa was obtained from the slope of the regression line (green line).

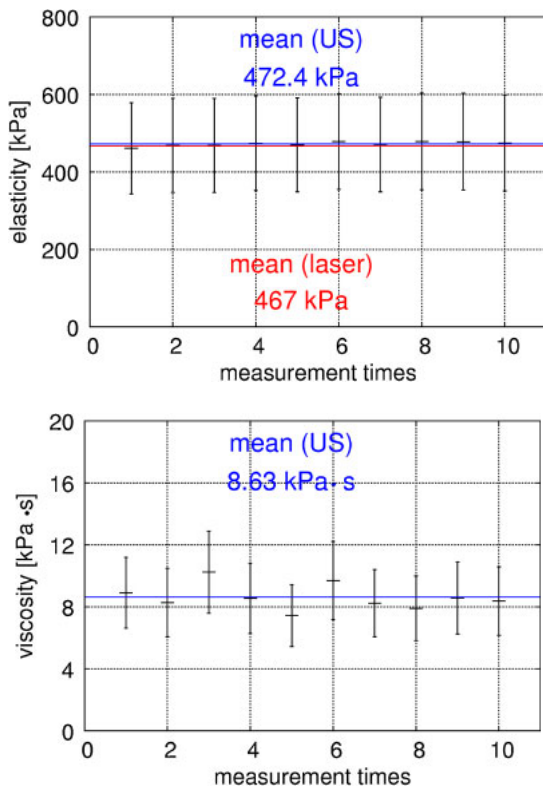


Fig. 8. (Color online) Means and standard deviations of measured elastic moduli and viscosity constants of the silicone tube. The red line shows the mean elasticity measured using a laser. The blue lines show the means of static elasticity and viscosity measured using ultrasound.

clearly decreased by adaptive LPF. In particular, the MSE obtained after the release of the cuff was decreased significantly.

Figure 11 shows the transient change in viscoelasticity due to FMD. After the release of the cuff, a temporal decrease in elasticity and a temporal increase in viscosity were measured. The transient changes in these parameters were similar to those in the previous study.²²⁾

4. Discussion

In this study, we evaluated the accuracy of the estimation of viscoelasticity by a basic experiment using a silicone tube

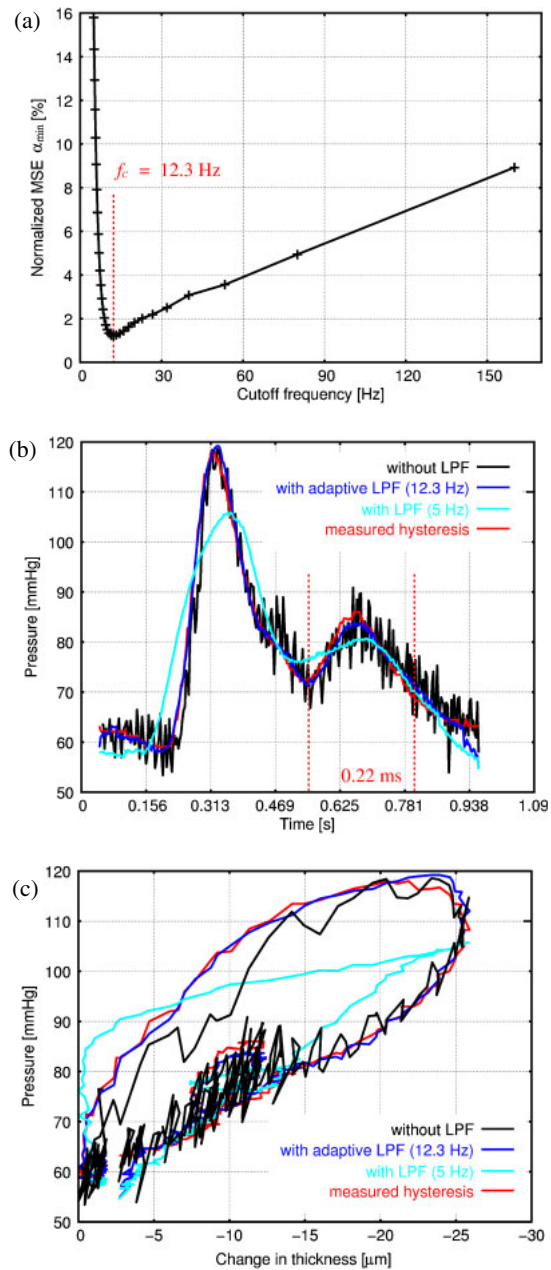


Fig. 9. (Color online) (a) Residual MSE α_{\min} at each cutoff frequency. (b) Estimated pressures obtained with and without filtering using adaptive cutoff frequency ($f_c = 12.3$ Hz). (c) Measured stress–strain relationships obtained and estimated stress–strain relationship with and without filtering.

(simulating artery). In Fig. 8, the elasticity is estimated with a small error (mean error of 1.2%, which is about 5 kPa). However, there are relatively large standard deviations. Figure 12 shows the elasticity measured at each beam position. As shown in Figs. 8 and 12, the measured elasticity values fluctuate among beams. However, the reproducibility of elasticity and the small fluctuation in elasticity are measured at the same position. Therefore, it is required that the variation in the viscoelasticity of the silicone tube should be further investigated. Moreover, the accuracy of the estimation of elasticity and reproducibility is demonstrated in this validation experiment.

Figure 9 shows the stress–strain relationship of the radial arterial wall during a heartbeat. As shown in Figs. 6(d) and

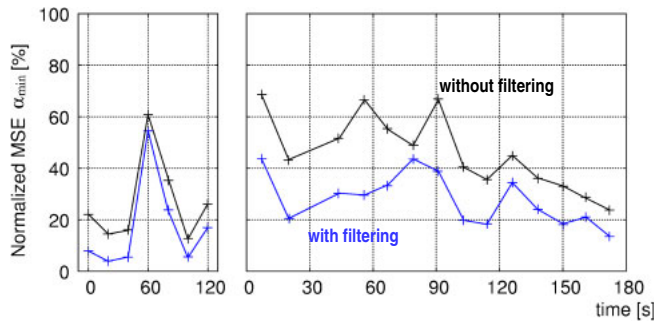


Fig. 10. (Color online) Transient change in α_{\min} for a healthy subject.

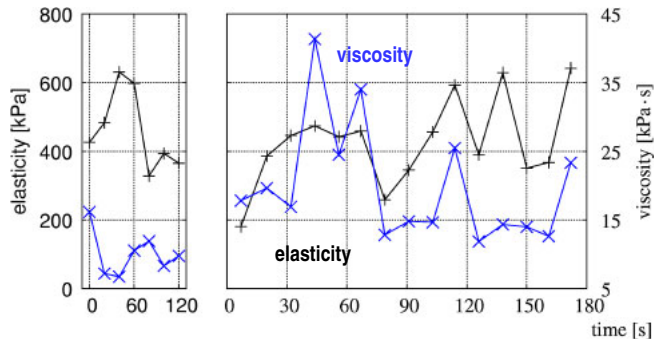


Fig. 11. (Color online) Transient change in viscoelasticity of the radial arterial wall due to FMD.

9(c), LPF decreases the high-frequency noise clearly and improves the accuracy in of the estimation of each parameter (corresponds to the shape of hysteresis). In particular, in the *in vivo* measurement, the inner small loop that corresponds to the negative pressure wave can be observed. Although the amplitude of this negative pressure wave is smaller than that of the positive pressure wave, it is an important component in vascular dynamics. The negative pressure wave is composed of high frequency components compared with the positive pressure wave. Therefore, the cutoff frequency of LPF should be determined not to remove the component of the negative pressure wave.

As shown in Fig. 9(c), the duration of the inner small loop is about 0.22 s [corresponds to the 2nd peak of blood pressure in Fig. 9(b) and the reciprocal of the duration is about 4.6 Hz]. Additionally, the main component of blood pressure waveform is about 1 Hz (corresponds to a cardiac cycle). The adaptive cutoff frequency is determined by evaluating the MSE using both components because such components are important in the arterial dynamics. As shown in the example in Fig. 9(a), the determined adaptive cutoff frequency is much higher (12.3 Hz) than 4.6 Hz to preserve the negative pressure component. As shown in Fig. 9(c), the estimated hysteresis loop is significantly deformed (at $f_c = 5$ Hz) when the cutoff frequency is not adaptively determined and is very low.

The shape of the stress–strain relationship includes much information. For example, the slope shows the elastic modulus, and the area depends on the ratio of the loss modulus to the static elastic modulus when the Voigt model is assumed. Therefore, the accurate measurement of the stress–strain relationship is very important for the detailed

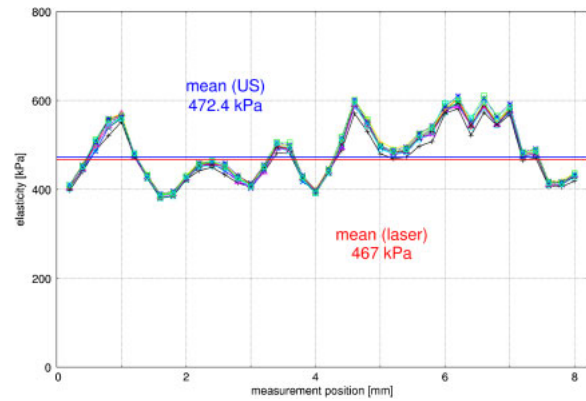


Fig. 12. (Color online) Mean elasticity measured at each beam position.

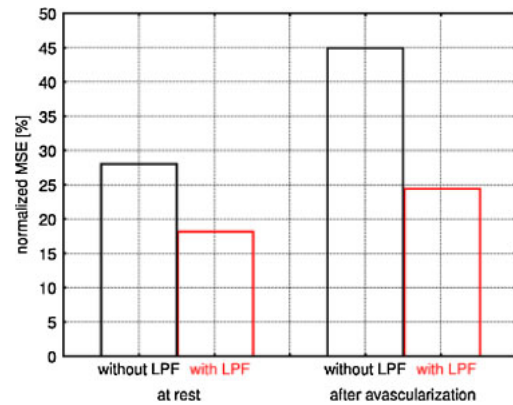


Fig. 13. (Color online) Means of α_{\min} obtained with and without LPF before and after avascularization.

analysis of viscoelasticity. Additionally, Fig. 13 shows the comparison of the means of α_{\min} obtained with and without LPF before and after avascularization. As shown in Figs. 10 and 13, the α_{\min} obtained after avascularization was larger than that obtained before avascularization. To evaluate FMD, stable measurements are necessary to evaluate the change in the viscoelasticity of the radial arterial wall. Therefore, the reduction in α_{\min} by LPF, particularly during FMD (after avascularization), significantly contributes to the measurement of the change in viscoelasticity.

5. Conclusions

In this study, we evaluated the accuracy of the estimation of viscoelasticity by a basic experiment using a silicone tube (simulating artery). In the basic experiment, the accuracy of reproducibility in the estimation of elasticity was demonstrated. Additionally, in the *in vivo* measurement, the normalized MSE α_{\min} was clearly decreased, and the inner small loop, which corresponds to the negative pressure wave caused by the closure of the aortic valve, was also observed by adaptive LPF. These results show the potential of the proposed method for the thorough analysis of the transient change in viscoelasticity due to FMD.

Acknowledgment

This work was supported by a Grant-in-Aid for JSPS Fellows (21-3796).

- 1) K. Tuzuki, H. Hasegawa, and H. Kanai: *Jpn. J. Appl. Phys.* **47** (2008) 4180.
- 2) D. G. Paeng, R. Y. Chiao, and K. K. Shung: *Ultrasound Med. Biol.* **30** (2004) 815.
- 3) N. Saitoh, H. Hasegawa, and H. Kanai: *Jpn. J. Appl. Phys.* **48** (2009) 07GJ08.
- 4) T. Fukushima, H. Hasegawa, and H. Kanai: *Jpn. J. Appl. Phys.* **50** (2011) 07HF02.
- 5) S. Satomura: *J. Acoust. Soc. Am.* **29** (1957) 1181.
- 6) H. Hasegawa and H. Kanai: *IEEE Trans. Ultrason. Ferroelectr. Freq. Control* **55** (2008) 2626.
- 7) R. Ross: *New Engl. J. Med.* **340** (1996) 115.
- 8) M. Walski, S. Chlopicki, R. Celary-walska, and M. Frontczak-baniewicz: *J. Physiol. Pharmacol.* **53** (2002) 713.
- 9) Y. Matsuzawa: *Nippon Rinsho* **51** (1993) 1951 [in Japanese].
- 10) A. E. Medvedev, V. I. Samsonov, and V. M. Fomin: *J. Méc. Théor. Appl.* **47** (2006) 324.
- 11) P. M. Vanhoutte: *J. Clin. Invest.* **107** (2001) 23.
- 12) D. S. Celermajer, K. E. Soresen, V. M. Gooch, D. J. Spiegelhalter, O. I. Miller, J. D. Sullivan, J. K. Lloyd, and J. E. Deanfield: *Lancet* **340** (1992) 1111.
- 13) M. C. Corretti, T. J. Anderson, E. J. Benjamin, D. Celermajer, F. Charbonneau, M. A. Creager, J. Deanfield, H. Drexler, M. Gerhard-Herman, D. Herrington, P. Vallance, J. Vita, and R. Vogel: *J. Am. Coll. Cardiol.* **39** (2002) 257.
- 14) J. Deanfield, A. Donald, C. Ferri, C. Giannattasio, J. Halcox, S. Halligan, A. Lerman, G. Mancina, J. J. Oliver, A. C. Pessina, D. Rizzoni, G. P. Rossi, A. Salvetti, E. L. Schiffrin, S. Taddei, and D. J. Webb: *J. Hypertension* **23** (2005) 7.
- 15) N. M. De Roos, M. L. Bots, E. G. Schouten, and M. B. Katan: *Ultrasound Med. Biol.* **29** (2003) 401.
- 16) M. Nishino: *Cho-onpa Igaku* **37** (2010) 243 [in Japanese].
- 17) D. R. Witte, J. Westerink, E. J. de Koing, Y. van der Graaf, D. E. Grobbee, and M. L. Bots: *J. Am. Coll. Cardiol.* **45** (2005) 1987.
- 18) P. C. Lavallee, P. Bonnin, J. Labreuche, P. Amarenco, and B. Lévy: *Ultrasound Med. Biol.* **32** (2006) 1165.
- 19) R. Ravikumar, R. Deepa, C. S. Shanthirani, and V. Mohan: *Am. J. Cardiol.* **90** (2002) 702.
- 20) T. Kaneko, H. Hasegawa, and H. Kanai: *Jpn. J. Appl. Phys.* **46** (2007) 4881.
- 21) M. Sugimoto, H. Hasegawa, and H. Kanai: *Jpn. J. Appl. Phys.* **44** (2005) 6297.
- 22) K. Ikeshita, H. Hasegawa, and H. Kanai: *Jpn. J. Appl. Phys.* **47** (2008) 4165.
- 23) K. Ikeshita, H. Hasegawa, and H. Kanai: *Jpn. J. Appl. Phys.* **48** (2009) 07GJ10.
- 24) K. Ikeshita, H. Hasegawa, and H. Kanai: *Jpn. J. Appl. Phys.* **50** (2011) 07HF08.
- 25) H. Kanai, M. Sato, Y. Koiwa, and N. Chubachi: *IEEE Trans. Ultrason. Ferroelectr. Freq. Control* **43** (1996) 791.